



## High-mobility group box 1 restores cardiac function after myocardial infarction in transgenic mice

メタデータ	<p>言語: English</p> <p>出版者: Oxford University Press</p> <p>公開日: 2010-06-08</p> <p>キーワード (Ja):</p> <p>キーワード (En): HMGB1, cardiac remodeling, angiogenesis, Animals, Coronary Vessels, HMGB1 Protein, Heart, Ligation, Mice, Mice, Transgenic, Myocardial Infarction, Myocardium, Myosin Heavy, Neovascularization, Physiologic, Promoter Regions, Genetic, Ventricular Myosins, Ventricular Remodeling</p> <p>作成者: Kitahara, Tatsuro, Takeishi, Yasuchika, Harada, Mutsuo, Niizeki, Takeshi, Suzuki, Satoshi, Sasaki, Toshiki, Ishino, Mitsunori, Bilim, Olga, Nakajima, Osamu, Kubota, Isao</p> <p>メールアドレス:</p> <p>所属:</p>
URL	<p><a href="https://fmu.repo.nii.ac.jp/records/2000010">https://fmu.repo.nii.ac.jp/records/2000010</a></p>

# High-mobility group box 1 restores cardiac function after myocardial infarction in transgenic mice

Tatsuro Kitahara, M.D.<sup>1</sup>, Yasuchika Takeishi, M.D.<sup>3</sup>, Mutsuo Harada, M.D.<sup>1</sup>, Takeshi Niizeki, M.D.<sup>1</sup>, Satoshi Suzuki, M.D.<sup>1</sup>, Toshiki Sasaki, M.D.<sup>1</sup>, Mitsunori Ishino, M.D.<sup>1</sup>, Olga Bilim, M.D.<sup>1</sup>, Osamu Nakajima, Ph.D.<sup>2</sup>, and Isao Kubota, M.D.<sup>1</sup>

<sup>1</sup>Department of Cardiology, Pulmonology and Nephrology, <sup>2</sup>Research Laboratory for Molecular Genetics, Yamagata University School of Medicine, Yamagata, and <sup>3</sup>First Department of Internal Medicine, Fukushima Medical University, Fukushima, Japan.

Short title: HMGB1 restores cardiac function after MI

Total word counts: 5436

Address for reprints: Yasuchika Takeishi, M.D.  
First Department of Internal Medicine  
Fukushima Medical University  
1 Hikarigaoka, Fukushima, Japan 960-1295  
E-mail: takeishi@fmu.ac.jp  
Phone: +81-24-547-1188 Fax: +81-24-548-1821

## ABSTRACT

**High-mobility group box 1 restores cardiac dysfunction after myocardial infarction in transgenic mice. Kitahara T, Takeishi Y, Harada M, Niizeki T, Suzuki S, Sasaki T, Bilim O, Nakajima O, Kubota I.**

**Aim:** High-mobility group box 1 (HMGB1) is a nuclear DNA-binding protein and is released from necrotic cells, inducing inflammatory responses and promoting tissue repair and angiogenesis. To test the hypothesis that HMGB1 enhances angiogenesis and restores cardiac function after myocardial infarction, we generated transgenic mice with cardiac specific overexpression of HMGB1 (HMGB1-Tg) using  $\alpha$ -myosin heavy chain (MHC) promoter. **Methods and Results:** The left anterior descending coronary artery was ligated in HMGB1-Tg and wild-type littermate (Wt) mice. After coronary artery ligation, HMGB1 was released into circulation from the necrotic cardiomyocytes of HMGB1 overexpressing hearts. The size of myocardial infarction was smaller in HMGB1-Tg than in Wt mice. Echocardiography and cardiac catheterization demonstrated that cardiac remodeling and dysfunction after myocardial infarction were prevented in HMGB1-Tg mice compared to Wt mice. Furthermore, survival rate after myocardial infarction of HMGB1-Tg mice was higher than that of Wt mice. Immunohistochemical staining revealed that capillary and arteriole formations after myocardial infarction were enhanced in HMGB1-Tg mice. **Conclusions:** We demonstrated the first in vivo evidence that HMGB1 enhances angiogenesis, restores cardiac function, and improves survival after myocardial infarction. These results may provide a novel therapeutic approach for left ventricular dysfunction after myocardial infarction.

**Key words:** HMGB1, cardiac remodeling, myocardial infarction, angiogenesis

## INTRODUCTION

High-mobility group box 1 (HMGB1) is a highly conserved, ubiquitous protein present in the nuclei of various types of cells<sup>1</sup>. HMGB1 has been identified as a nuclear DNA-binding protein, which participates in maintaining nucleosome structure, regulating gene transcription, and modulating the activity of steroid hormone receptors<sup>2</sup>.<sup>3</sup>. This protein is essential for survival, since HMGB1-deficient mice die due to hypoglycemia within 24 hrs after birth<sup>4</sup>. On the other hand, recent studies have demonstrated that HMGB1 is secreted into the extracellular milieu from necrotic and inflammatory cells, but not apoptotic cells, and acts as a cytokine with multiple functions<sup>5</sup>. HMGB1 has been reported to transduce cellular signals by interacting with at least three receptors: receptor for advanced glycation end products (RAGE), Toll-like receptor (TLR)-2 and TLR-4<sup>4</sup>. Signaling through these receptors leads to activation of the nuclear factor- $\kappa$ B (NF- $\kappa$ B), extra-cellular signal regulated kinase and p38 mitogen activated protein kinase<sup>6-7</sup>. Thus once released, HMGB1 mediates various cellular responses including cell migration, release of pro-inflammatory cytokines, tissue repair, and angiogenesis<sup>4, 6, 7</sup>.

Myocardial infarction is an irreversible injury, caused by the occlusion of a coronary artery, leading to cardiomyocyte death, tissue loss, and scar formation. Angiogenesis, the growth of new blood vessels from pre-existing ones, plays an important role in various pathological settings, including tumor growth, wound repair, and myocardial infarction<sup>8</sup>. Various cytokines and chemokines exert a proangiogenic activity by acting directly on endothelial cells or indirectly by inducing the production of angiogenic growth factors<sup>9</sup>. Recent studies have demonstrated that HMGB1 exerts

proangiogenic effects by cell proliferation, chemotaxis, migration, and sprouting of endothelial cells in vitro<sup>6, 10</sup>.

Based on these findings, we hypothesized that HMGB1 enhanced angiogenesis and restored cardiac function after myocardial infarction. To test this hypothesis, we generated transgenic mice with cardiac specific overexpression of HMGB1 using  $\alpha$ -myosin heavy chain (MHC) promoter. We examined cardiac function, survival, and capillary formation after coronary artery ligation in mice. Our present results show that HMGB1 enhances capillary and arteriole formation, prevents cardiac remodeling, restores cardiac function, and improves survival after myocardial infarction in vivo.

## METHODS

### *Generation of HMGB1 transgenic mice*

All experimental procedures were performed according to the animal welfare regulations of Yamagata University School of Medicine, and the study protocol was approved by the Animal Subjects Committee of Yamagata University School of Medicine. The investigation conformed to the Guide for the Care and Use of Laboratory Animals published by the US National Institutes of Health. Transgenic mice with cardiac-specific overexpression of HMGB1 (HMGB1-Tg) were created in our laboratory by standard techniques as reported previously<sup>11-14</sup>. Briefly, a 5.5-kb fragment of murine  $\alpha$ -MHC gene promoter (a kind gift from Dr. J. Robbins, Children's Hospital Research Foundation, Cincinnati, Ohio) and 0.7-kb human HMGB1 cDNA<sup>15</sup> (a kind gift from Drs. I. Maruyama and K. Abeyama, Kagoshima University Faculty of Medicine, Kagoshima, Japan) were subcloned into pGEX-5X-1 plasmids. The plasmid was digested with SpeI to generate a DNA fragment composed of the  $\alpha$ -MHC gene promoter, HMGB1 cDNA, and a poly A tail of the human growth hormone. We microinjected the construct into the pronuclei of single-cell fertilized mouse embryos to generate transgenic mice as previously described<sup>11-14</sup>. To detect the exogenous HMGB1 gene, genomic DNA was extracted from the tail tissues of 3- to 4-week-old pups, and polymerase chain reaction (PCR) was performed with one primer specific for the  $\alpha$ -MHC gene promoter and another primer specific for the HMGB1<sup>14</sup>. Wild type littermate mice (Wt) were used as control.

### *Surgery of left anterior descending coronary artery ligation*

Surgeon was kept unaware of the results of the genotype, and the animal surgeries were performed by the same surgeon. Induction of myocardial infarction (MI) was performed in 8- to 10-weeks-old mice as described previously<sup>16, 17</sup>. Briefly, mice (20 to 25 g body weight) were anesthetized by intraperitoneal injection with a mixture of ketamine (80 mg/kg) and xylazine (8 mg/kg). Animals were intubated with a 20-gauge polyethylene catheter and were ventilated with a rodent ventilator (Harvard Apparatus, Holliston, MA, USA). An incision was performed along the left sternal border, and the fourth rib was cut proximal to the sternum. The left anterior descending coronary artery was identified, and an 8-0 proline suture was passed around the artery and subsequently tied off. Successful ligation of the coronary artery was verified visually by the discoloration of the left ventricular myocardium. In sham-operated animals, the same procedure was performed except the coronary artery ligation. Finally, the heart was repositioned in the chest, and the chest wall was closed. The animals remained in a supervised setting until fully conscious.

### ***Echocardiography and cardiac catheterization***

Transthoracic echocardiography was recorded under anesthesia with an intraperitoneal injection of pentobarbital sodium (35 mg/kg) as described previously with an FFsonic 8900 (Fukuda Denshi Co., Tokyo, Japan) equipped with a 13-MHz phased-array transducer<sup>14, 16-18</sup>. Left ventricular internal dimensions at end-systole and end-diastole (LVESD and LVEDD), wall thickness of inter-ventricular septum (IVS), and left ventricular posterior wall (PW) were measured digitally on the M-mode tracings and averaged from at least 3 cardiac cycles. Left ventricular fractional shortening (LVFS) was calculated as  $[(LVEDD-LVESD)/LVEDD] \times 100 (\%)$ .

A closed-chest approach by cardiac catheter was performed to evaluate hemodynamic parameters as described previously<sup>19, 20</sup>. The right carotid artery was cannulated under anesthesia with an intraperitoneal injection of pentobarbital sodium (35 mg/kg) by the micro-pressure transducers with an outer diameter of 0.42 mm (Samba 3200, Samba Sensors AB, Göteborg, Sweden), which was then advanced into the left ventricle. Heart rate, left ventricular peak systolic pressure (LVSP), end-diastolic pressure (LVEDP), developed pressure (LVDP), maximal and minimum rates of left ventricular pressure development (max and min  $dP/dt$ , respectively), and time constant of left ventricular isovolumic relaxation (Tau) were measured using an Acknowledge version 3.8.1 system with a sampling rate of 500 Hz<sup>(19, 20)</sup>.

### ***Western blotting***

Total proteins were extracted from the left ventricle with ice-cold lysis buffer as described previously<sup>21-23</sup>. Protein concentration of myocardial samples was carefully determined by the protein assay (Bio-Rad Laboratories, Inc., Hercules, CA, USA). Equal amounts of protein were subjected to 10% SDS-PAGE electrophoresis and transferred to polyvinylidene difluoride (PVDF) membranes. To ensure equivalent protein loading and quantitative transfer efficiency of proteins, membranes were stained with Ponceau S before incubating with primary antibodies. Antibodies used in this study were a rabbit polyclonal anti-HMGB1 antibody (Shino-Test Corporation, Sagamihara, Japan), a mouse monoclonal anti-glyceraldehyde-3-phosphate dehydrogenase (GAPDH) antibody (Chemicon International, Inc., Temecula, CA, USA) and anti- $\beta$ -actin antibody (SIGMA, Saint Louis, MO, USA). Immunoreactive bands were detected by an ECL kit (Amersham Biosciences,



Piscataway, NJ, USA), and cardiac HMGB1 expression was normalized to GAPDH or  $\beta$ -actin.

### ***Histopathological examinations***

At 4 weeks after surgery, mice were sacrificed, coronary arteries were retrogradely flushed with saline, and the heart was excised and weighed. The heart was fixed with a 2% solution of paraformaldehyde in PBS at 4 °C for 30 min, and then sequentially in 10%, 20%, 30% sucrose in PBS, respectively, for 4 hours. Then three transverse slices from the base, mid-region, and apex of the left ventricle were embedded and frozen in optimal cutting temperature compound. These three sections were stained with Masson-trichrom stain. In each left ventricular transverse section, the infarct length was calculated by measuring the endocardial and epicardial surface length delimiting the infarcted region<sup>16, 17</sup>. Percent infarct size was calculated as infarct length divided by the total left ventricular circumference. Some mice were analyzed for initial area at risk (AAR) by injection of Evans blue dye. Briefly, after ligation of the left anterior descending coronary artery, 0.5 ml of 1.0 % Evans blue dye was injected through the inferior vena cava to delineate the nonischemic tissue. We then excised the heart, washed with PBS and cut into three transverse slices. We determined left ventricular area and area at risk by computerized planimetry using Image J software (version 1.38x, National Institutes of Health). We expressed initial area at risk as a percentage of the left ventricular area.

In immunohistochemical analysis, anti-platelet endothelial cell adhesion molecule (PECAM) antibody (rat monoclonal anti-PECAM antibody, Cedarlane Laboratories Limited, Ontario, Canada) was used to identify endothelial cells with

avidinbiotinylated peroxidase complex (Vector Laboratories, Burlingame, CA, USA). The staining was visualized by treatment for 15-20 seconds in the solution of 3, 3'-diaminobenzidine (Dako Japan, Tokyo, Japan). Sections were counterstained with hematoxylin to identify nucleus. We also used alkaline phosphatase anti- $\alpha$  smooth muscle actin ( $\alpha$ SMA) antibody (SIGMA, Saint Louis, MO, USA) to identify  $\alpha$  smooth muscle actin positive vessels. The staining was visualized by the solution of 5-bromo-4-chloro-3-indolylphosphate/nitro blue tetrazolium (SIGMA, Saint Louis, MO, USA). Sections were counterstained with nuclear fast red solution to identify nucleus. Control reactions included the omission of the primary antibody, which was substituted by nonimmune rabbit serum. We examined the numbers of PECAM-positive cells and  $\alpha$ SMA-positive cells in light-microscopic sections taken from the border zone (1 to 2 mm from the edge of infarction zone) at 4 weeks after MI. Ten random microscopic fields in the border zone were examined, the numbers of PECAM-positive cells/high power field (HPF, magnification  $\times$  400) and  $\alpha$ SMA-positive cells/HPF were counted, and the data from 10 fields were averaged<sup>(24)</sup>. For double immune staining, the sections were stained with phycoerythrin conjugated anti-mouse PECAM-1 antibody (eBioscience, Inc., San Diego, CA, USA) and FITC conjugated anti-mouse  $\alpha$ SMA antibody (SIGMA, Saint Louis, MO, USA). Fluorescence image stacks were acquired at emission wavelengths of 515 and 480 nm, respectively.

### ***ELISA***

Plasma levels of HMGB1 were measured by a commercially available ELISA kit (Shino-Test Corporation, Sagami-hara, Japan) in Wt and HMGB1-Tg mice.

### ***Statistical Analysis***

All values are expressed as mean  $\pm$  SE. Comparisons between Wt and HMGB1-TG mice were performed by the Mann-Whitney's U test. Effects of MI on heart weight, histological, echocardiographic, and hemodynamic findings in each animal group were analyzed by two-way ANOVA followed by multiple comparisons with a Bonferroni test. Survival curves after MI were created by the Kaplan-Meier method and compared by a log rank test. A value of  $P < 0.05$  was considered statistically significant.

## RESULTS

### *Generation of HMGB1-Tg mice*

After microinjection and embryo implantation, HMGB1-Tg mice were successfully established, and cardiac-specific expression of transgene was confirmed by reverse transcriptase-PCR (Figure 1A). We could generate only one line of HMGB1-TG mouse. Protein level of HMGB1 was augmented approximately 4-fold in HMGB1-Tg mouse hearts compared to Wt as shown in Figure 1B. Immunohistochemical staining with HMGB1 demonstrated that HMGB1 localized in the nucleus, and strong staining in the nucleus was observed in cardiomyocytes of HMGB1-Tg mice compared to Wt mice as shown in Figure 1C. However, there was no significant difference in plasma level of HMGB1 between Wt and HMGB1-Tg mice at basal condition (under the assay sensitivity respectively,  $< 0.2$  ng/ml). No neonatal and adult deaths were observed in HMGB1-Tg mice. There were no significant differences in gravimetric data and cardiac function at basal condition between Wt and HMGB1-Tg mice as reported in Table 1.

### *Changes in cardiac and plasma concentrations of HMGB1 after myocardial infarction*

Cardiac HMGB1 levels were examined by Western blotting at 24 hrs after MI. In the infarct zone, HMGB1 level decreased markedly ( $P < 0.01$ ) in HMGB1-Tg mice compared to sham-operated mice (Figure 2A). In the non-infarct zone, there was no significant change in cardiac HMGB1 level after MI.

We also measured plasma concentrations of HMGB1 before MI and at 12, 24,

48 hrs after MI by ELISA. Plasma HMGB1 levels after MI were significantly increased in both Wt and HMGB1-Tg mice. In particular, plasma HMGB1 level in HMGB1-Tg mice at 24 hrs after MI was significantly increased than that in Wt mice as shown in Figure 2B ( $P < 0.01$ ). These data suggest that HMGB1 was pronouncedly released into circulation from necrotic cardiomyocytes in HMGB1-Tg mice compared to Wt mice.

### ***Left ventricular remodeling and cardiac function after myocardial infarction***

There was no significant difference in the ratio of heart weight to body weight in the sham-operated Wt and HMGB1-Tg mice (Figure 3). At 4 weeks after MI, the ratio of heart weight to body weight was significantly increased in Wt mice ( $P < 0.01$ ). However, increase in the ratio of heart weight to body weight after MI was significantly attenuated in HMGB1-Tg mice compared to Wt mice ( $P < 0.05$ ) as demonstrated in Figure 3A.

The percent infarct size was compared between Wt and HMGB1-Tg mice. As shown in Figure 3B, the percent infarct size at 4 weeks after MI was significantly smaller in HMGB1-Tg mice than in Wt mice ( $P < 0.05$ ). Initial AAR was evaluated by injection of Evans blue dye after ligation of coronary artery. However, there was no difference in size of initial AAR between Wt and HMGB1-Tg mice ( $58.4 \pm 1.4\%$  vs.  $59.3 \pm 1.6\%$ ).

We examined cardiac function of Wt and HMGB1-Tg mice by echocardiography and cardiac catheterization at 4 weeks after MI. Echocardiography demonstrated that LVEDD and LVESD were significantly smaller ( $P < 0.01$ ) and LVFS was significantly higher ( $P < 0.01$ ) in HMGB1-Tg mice than in Wt mice at 4 weeks

after MI (Figure 4A and Table 2). IVS thinning was also attenuated in HMGB1-Tg mice compared to Wt mice ( $P < 0.01$ ). As shown in Figure 4B and Table 2, hemodynamic assessment by cardiac catheterization revealed that LVDP, max dP/dt, and min dP/dt were significantly higher in HMGB1-Tg mice than in Wt mice ( $P < 0.05$ ) at 4 weeks after MI. Furthermore, LVEDP was significantly lower ( $P < 0.01$ ) and Tau was significantly shorter ( $P < 0.05$ ) in HMGB1-Tg mice compared to Wt mice at 4 weeks after MI. These data suggest that cardiac systolic and diastolic function at 4 weeks after MI was preserved in HMGB1-Tg mice compared to Wt mice.

#### ***HMGB1 improved survival rates after myocardial infarction***

The survival rates from recovery of MI surgery were compared up to 4 weeks among Wt sham, HMGB1-Tg sham, Wt MI and HMGB1-TG MI groups (Figure 5). The survival rate up to 4 weeks after MI was significantly higher in HMGB1-Tg mice than in Wt mice (69% vs. 38%,  $P < 0.01$ ).

#### ***Capillary and arteriole densities in the border zone***

We examined the numbers of PECAM-positive cells and  $\alpha$ SMA-positive cells in light-microscopic sections taken from the border zone (1 to 2 mm from the edge of infarction zone) at 4 weeks after MI (Figure 6). Numbers of PECAM-positive cells and  $\alpha$ SMA-positive cells were greater in HMGB1-Tg than in Wt mice ( $P < 0.01$  and  $P < 0.05$ , respectively). Although  $\alpha$ SMA protein was reported expressing in myofibroblasts in the infarcted heart (25), double immune staining for PECAM and  $\alpha$ SMA revealed that numbers of  $\alpha$ SMA-positive cells with PECAM-positive cells were greater in HMGB1-Tg than in Wt mice (Figure 6C). These data suggest that capillary

and arteriole densities were increased after MI in HMGB1-Tg mice.

## DISCUSSION

After coronary artery ligation, HMGB1 was released into circulation from the necrotic cardiomyocytes of HMGB1 overexpressing hearts. The size of myocardial infarction was smaller in HMGB1-Tg than in Wt mice. Echocardiography and cardiac catheterization demonstrated that cardiac remodeling and dysfunction after myocardial infarction were prevented in HMGB1-Tg mice compared to Wt mice. Furthermore, survival rate after myocardial infarction of HMGB1-TG mice was higher than that of Wt mice. Immunohistochemical staining revealed that capillary and arteriole formations were enhanced in HMGB1-Tg mice.

HMGB1, a 215 amino acid protein, was identified as chromosomal protein with important structural functions in chromatin organization<sup>1-3</sup>. HMGB1 is ubiquitously present in all vertebrate nuclei with a uniquely conserved sequence among species. HMGB1 binds double-stranded DNA and interacts with other DNA binding proteins, which facilitate chromatin bending<sup>3</sup>. This architectural function facilitates the binding of several transcriptional factors including some steroid hormone receptors. HMGB1-deficient mice die within a few hours from birth, possibly as a result of a defect in activation of glucocorticoid receptor-responsive genes<sup>26</sup>.

The novel function of HMGB1 as a cytokine originates from studies of endotoxemia and sepsis<sup>27</sup>. HMGB1 acts as a late mediator of lipopolysaccharide (LPS) lethality. HMGB1 is released from a variety of cells including macrophages, pituicytes, peripheral blood mononuclear cells, and necrotic cells<sup>4-7</sup>. Serum concentrations of HMGB1 increase significantly after administration of LPS or tumor necrosis factor- $\alpha$  in mice<sup>27</sup>. Effects of the extracellular HMGB1 are mediated by its



binding to the RAGE, TLR-2 and TLR-4. Interaction of HMGB1 with RAGE or TLR induces pro-proliferative effects for vessel-associated stem cells<sup>28</sup>. Recently, Limana et al. have demonstrated that exogenously administered HMGB1 protein in the peri-infarcted left ventricle elicits myocardial regeneration from resident cardiac c-Kit<sup>+</sup> progenitor cells<sup>29</sup>. Chavakis et al. have recently reported that HMGB1 activates integrin-dependent homing of endothelial progenitor cells to ischemic tissues<sup>30</sup>. Mitola et al. have demonstrated that RAGE blockade inhibits HMGB1-induced neovascularization and endothelial cell proliferation in vitro<sup>6</sup>. These data support our present findings that capillary and arteriole formations after myocardial infarction were enhanced in transgenic mouse hearts overexpressing HMGB1 (Figure 6). As demonstrated in Figure 2, HMGB1 was released from the necrotic cardiomyocytes and might enhance angiogenesis by paracrine and autocrine mechanisms. Consequently, the size of myocardial infarction, IVS thinning and the ratio of heart weight to body weight after myocardial infarction were reduced in HMGB1-Tg mice (Figure 3). Cardiac function after myocardial infarction was restored (Figures 4), and survival rate was improved (Figure 5) in HMGB1-Tg mice. Recently, the importance of cardiac angiogenesis has been reported in pressure overload-induced cardiac dysfunction<sup>31</sup>.

In the present study, we could analyze only one line of HMGB1-Tg mice because of breeding problem. Ideally, effects of HMGB1 on angiogenesis and cardiac function should be examined in multiple transgenic mouse lines with different expression levels in the heart.

## ***Conclusions***

We demonstrated the first in vivo evidence that HMGB1 enhances

angiogenesis, restores cardiac function, and improves survival after myocardial infarction. These results may provide a novel potential strategy to prevent cardiac remodeling and improve cardiac function and survival for patients with ischemic disorders.

### ***Funding***

This study was supported in part by a grant-in-aid for Scientific Research (Nos. 18590760 and 19590804) from the Ministry of Education, Science, Sports and Culture, Japan, and grants from the Takeda Science Foundation and Fukuda Foundation for Medical Technology.

### ***Conflict of Interest***

None

## REFERENCES

1. Andersson U, Erlandsson-Harris H, Yang H, Tracey KJ. HMGB1 as a DNA-binding cytokine. *J Leukoc Biol* 2002; **72**: 1084-1091.
2. Goodwin GH, Sanders C, Johns EW. A new group of chromatin-associated proteins with a high content of acidic and basic amino acids. *Eur J Biochem* 1973; **38**: 14-17.
3. Bianchi ME, Beltrame M. Upwardly mobile proteins. The role of HMG proteins in chromatin structure, gene expression and neoplasia. *EMBO* 2000; **Rep.1**: 109-119.
4. Lotze MT, Tracey KJ. High-mobility group box 1 protein (HMGB1): Nuclear weapon in the immune arsenal. *Nat Rev Immunol* 2005; **5**: 331-342.
5. Yang H, Wang H, Czura CJ, Tracey KJ. The cytokine activity of HMGB1. *J Leukoc Biol* 2005; **78**: 1-8.
6. Mitola S, Belleri M, Urbinati C, Coltrini D, Sparatore B, Pedrazzi M, et al. Cutting Edge: Extracellular high mobility group box-1 protein is a proangiogenic cytokine. *J Immunol* 2006; **176**: 12-15.
7. Yamada S, Maruyama I. HMGB1, a novel inflammatory cytokine. *Clinica Chimica Acta* 2007; **375**: 36-42.
8. Carmeliet P, Jain RK. Angiogenesis in cancer and other diseases. *Nature* 2000; **407**: 249-257.
9. Bernardini G, Ribatti D, Spinetti G, Morbidelli L, Ziche M, Santoni A et al. Analysis of the role of chemokines in angiogenesis. *J Immunol Methods* 2003; **273**: 83-101.

10. Schlueter C, Weber H, Meyer B, Rogalla P, Roeser K, Hauke S *et al.* Angiogenic signaling through hypoxia. HMGB1: An angiogenetic switch molecule. *Am J Pathol* 2005; **166**: 1259-1263.
11. Gordon JW, Scangos GA, Plotkin DJ, Barbosa JA, Ruddle FH. Genetic transformation of mouse embryos by microinjection of purified DNA. *Proc Natl Acad Sci U S A* 1980; **77**: 7380-7384.
12. Takeishi Y, Chu G, Kirkpatrick DL, Wakasaki H, Li Z *et al.* In vivo phosphorylation of cardiac troponin I by PKC $\beta$ 2 decreases cardiomyocyte calcium responsiveness and contractility in transgenic mouse heart. *J Clin Invest* 1998; **102**: 72-78.
13. Takeishi Y, Ping P, Bolli R, Kirkpatrick DL, Hoit BD, Walsh RA. Transgenic overexpression of constitutively active protein kinase C- $\epsilon$  causes concentric cardiac hypertrophy. *Circ Res* 2000; **86**: 1218-1223.
14. Arimoto T, Takeishi Y, Takahashi H, Shishido T, Tsunoda Y, Niizeki T *et al.* Cardiac-specific overexpression of diacylglycerol kinase  $\zeta$  prevents Gq protein coupled receptor agonist-induced cardiac hypertrophy in transgenic mice. *Circulation* 2006; **113**: 60-66.
15. Abeyama K, Stern DM, Ito Y, Kawahara K, Yoshimoto Y, Tanaka M *et al.* The N-terminal domain of thrombomodulin sequesters high-mobility group-B1 protein, a novel anti-inflammatory mechanism. *J Clin Invest* 2005; **115**: 1267-1274.
16. Shishido T, Nozaki N, Yamaguchi S, Nitobe J, Miyamoto T, Takahashi H *et al.* Toll-like receptor-2 modulates ventricular remodeling after myocardial infarction. *Circulation* 2003; **108**: 2905-2910.

17. Niizeki T, Takeishi Y, Arimoto T, Takahashi H, Shishido T, Koyama Y *et al.* Diacylglycerol kinase  $\zeta$  attenuates left ventricular remodeling and improves survival after myocardial infarction. *Am J Physiol Heart Circ Physiol* 2007; **292**: H1105-1112.
18. Nozaki N, Shishido T, Takeishi Y, Kubota I. Modulation of doxorubicin-induced cardiac dysfunction in Toll-like receptor 2 knockout mice. *Circulation* 2004; **110**: 2869-2874.
19. Zhai P, Yamamoto M, Galeotti J, Liu J, Masurekar M, Thaisz J *et al.* Cardiac-specific overexpression of AT1 receptor mutant lacking G  $\alpha_q$ /G  $\alpha_i$  coupling causes hypertrophy and bradycardia in transgenic mice. *J Clin Invest* 2005; **115**: 3045-3056.
20. Niizeki T, Takeishi Y, Koyama Y, Kitahara T, Suzuki S, Mende U *et al.* Diacylglycerol kinase- $\zeta$  rescues  $G\alpha_q$ -induced heart failure. *Circ J* 2008; **72**: 309-317.
21. Takeishi Y, Abe J, Lee JD, Kawakatsu H, Walsh RA, Berk BC. Differential regulation of p90 ribosomal S6 kinase and big mitogen-activated protein kinase-1 by ischemia/reperfusion and oxidative stress in perfused guinea pig hearts. *Circ Res* 1999; **85**: 1164-1172.
22. Takeishi Y, Huang Q, Abe J, Glassman M, Che W, Lee JD *et al.* Src and multiple MAP kinase activation in cardiac hypertrophy and congestive heart failure under chronic pressure-overload: comparison with acute mechanical stretch. *J Mol Cell Cardiol* 2001; **33**: 1637-1648.
23. Takahashi H, Takeishi Y, Miyamoto T, Shishido T, Arimoto T, Konta T *et al.* Protein kinase C and extracellular signal regulated kinase are involved in cardiac

- hypertrophy of rats with progressive renal injury. *Eur J Clin Invest* 2004; **34**: 85-93.
24. Cho SW, Moon SH, Lee SH, Kang SW, Kim J, Lim JM *et al.* Improvement of postnatal neovascularization by human embryonic stem cell derived endothelial-like cell transplantation in a mouse model of hindlimb ischemia. *Circulation* 2007; **116**: 2409-2419.
  25. Morimoto H, Takahashi M, Izawa A, Ise H, Hongo M, Kolattukudy PE *et al.* Cardiac overexpression of monocyte chemoattractant protein-1 in transgenic mice prevents cardiac dysfunction and remodeling after myocardial infarction. *Circ Res* 2006; **99**: 891-899.
  26. Calogero S, Grassi F, Aguzzi A, Voigtlander T, Ferrier P, Ferrari S *et al.* The lack of chromosomal protein Hmg1 does not disrupt cell growth but causes lethal hypoglycemia in newborn mice. *Nat Genet* 1999; **22**: 276-280.
  27. Wang H, Bloom O, Zhang M, Vishnubhakat JM, Ombrellino M, Che J *et al.* HMG-1 as a late mediator of endotoxin lethality in mice. *Science* 1999; **285**: 248-251.
  28. Palumbo R, Sampaolesi M, De Marchis F, Tonlorenzi R, Colombetti S, Mondino A *et al.* Extracellular HMGB1, a signal of tissue damage, induces mesoangioblast migration and proliferation. *J Cell Biol* 2004; **164**: 441-449.
  29. Limana F, Germani A, Zacheo A, Kajstura J, Carlo AD, Borsellino G *et al.* Exogenous high-mobility group box 1 protein induces myocardial regeneration after infarction via enhanced cardiac c-Kit<sup>+</sup> cell proliferation and differentiation. *Circ Res* 2005; **97**: e73-e83.

30. Chavakis E, Hain A, Vinci M, Carmona G, Bianchi ME, Vajkoczy P *et al.* High-mobility group box 1 activates integrin-dependent homing of endothelial progenitor cells. *Circ Res* 2007; **100**: 204-212.
31. Sano M, Minamino T, Toko H, Miyauchi H, Orimo M, Qin Y *et al.* p53-induced inhibition of Hif-1 causes cardiac dysfunction during pressure overload. *Nature* 2007; **446**: 444-448.

## FIGURE LEGENDS

### Figure 1. Generation of HMGB1-Tg mice

- (A) RNA was extracted from brain, heart, lung, liver, spleen, kidney, skeletal muscle and intestine tissues of HMGB1-Tg mice, and cardiac-specific expression of transgene was confirmed by RT-PCR.
- (B) HMGB1 protein expression in the left ventricle of Wt and HMGB1-Tg mice was examined by Western blotting. Protein level of HMGB1 was augmented about 4-fold in HMGB1-Tg hearts compared to Wt littermates.  $**P < 0.01$  vs. Wt mice (n = 5).
- (C) Localization of HMGB1 in cardiomyocytes of Wt and HMGB1-Tg mice. HMGB1 was localized in the nuclei of cardiomyocytes. Scale bars, 100  $\mu$ m on low-power field and 10  $\mu$ m on high-power field.

### Figure 2. Concentrations of HMGB1 in the heart and peripheral blood after myocardial infarction.

- (A) HMGB1 protein expressions in the left ventricle at 24 hrs after MI were examined by Western blotting. In the infarct zone, HMGB1 protein level reduced markedly at 24 hrs after coronary artery ligation compared with sham-operated HMGB1-Tg mice. MI, myocardial infarction; IZ, infarct zone; NIZ, non-infarct zone.  $**P < 0.01$  vs. Wt mice and  $^{##}P < 0.01$  vs. Tg sham (n = 6).
- (B) Plasma levels of HMGB1 at several time intervals after MI. Plasma HMGB1 levels increased significantly in HMGB1-Tg mice after MI.  $^{\#}P < 0.05$ ,  $^{##}P < 0.01$  vs. preoperative mice and  $**P < 0.01$  vs. Wt mice at 24 hrs after MI (n = 6 for each).



**Figure 3. Heart weight and infarct size in HMGB1-Tg and Wt mice.**

- (A) Ratio of heart to body weight at 4 weeks after MI. Increase of heart to body weight ratio after MI was attenuated in HMGB1-Tg mice compared to Wt mice.  $**P < 0.01$  vs. WT sham and  $\#P < 0.05$  vs. Wt MI mice ( $n = 8-10$ ).
- (B) Masson trichrome staining of the heart at 4 weeks after MI. The infarct size after MI was significantly smaller in HMGB1-Tg mice than in Wt mice.  $*P < 0.05$  vs. Wt mice ( $n = 10$ ). Scale bar, 1 mm.

**Figure 4. Echocardiography and hemodynamic data at 4 weeks after myocardial infarction.**

- (A) Representative M-mode recordings at 4 weeks after MI. HMGB1-Tg mice showed smaller LVEDD and higher LVFS than Wt mice after MI.
- (B) Representative left ventricular (LV) pressure recordings at 4 weeks after MI. HMGB1-Tg mice showed higher LVDP and lower LVEDP than Wt mice after MI.

**Figure 5. Survival rates after myocardial infarction.**

Survival curves up to 4 weeks after MI were created by a Kaplan-Meier method and compared by a log-rank test. Survival rates were significantly higher in HMGB1-Tg mice than in Wt mice after MI.  $**P < 0.01$  vs. Wt mice.

**Figure 6. Capillary and arteriole densities after myocardial infarction.**

- (A) Immunohistochemical staining with anti-PECAM antibody in the border zone of the heart at 4 weeks after MI. The numbers of PECAM-positive cells were counted and shown in the bar graph. The numbers of PECAM-positive cells were greater

in HMGB1-Tg mice than in Wt mice.  $**P < 0.01$  vs. Wt mice ( $n = 10$ ). Scale bar, 50  $\mu\text{m}$ .

**(B)** Immunohistochemical staining with anti- $\alpha$ SMA antibody in the border zone of the heart at 4 weeks after MI. The number of  $\alpha$ SMA-positive cells were counted and shown in the bar graph.  $\alpha$ SMA-positive cells after MI were more frequently observed in HMGB1-Tg mice than in Wt mice.  $*P < 0.05$  vs. Wt mice ( $n = 10$ ). Scale bar, 100  $\mu\text{m}$ .

**(C)** Double immunohistochemical staining with anti-PECAM antibody and anti- $\alpha$ SMA antibody in the border zone of the heart at 4 weeks after MI. Red fluorescence, PECAM; green fluorescence,  $\alpha$ SMA; Scale bars, 100  $\mu\text{m}$  on low-power field and 50  $\mu\text{m}$  on high-power field.

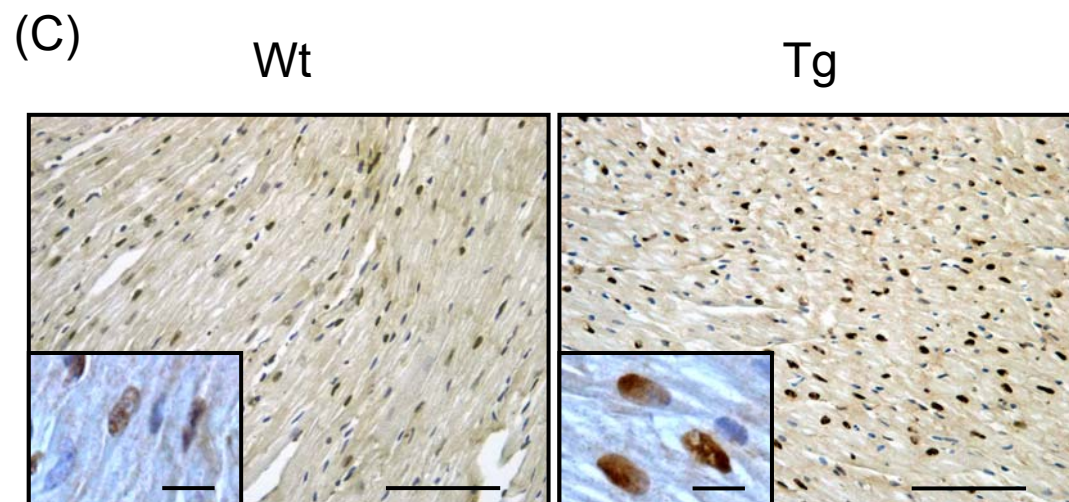
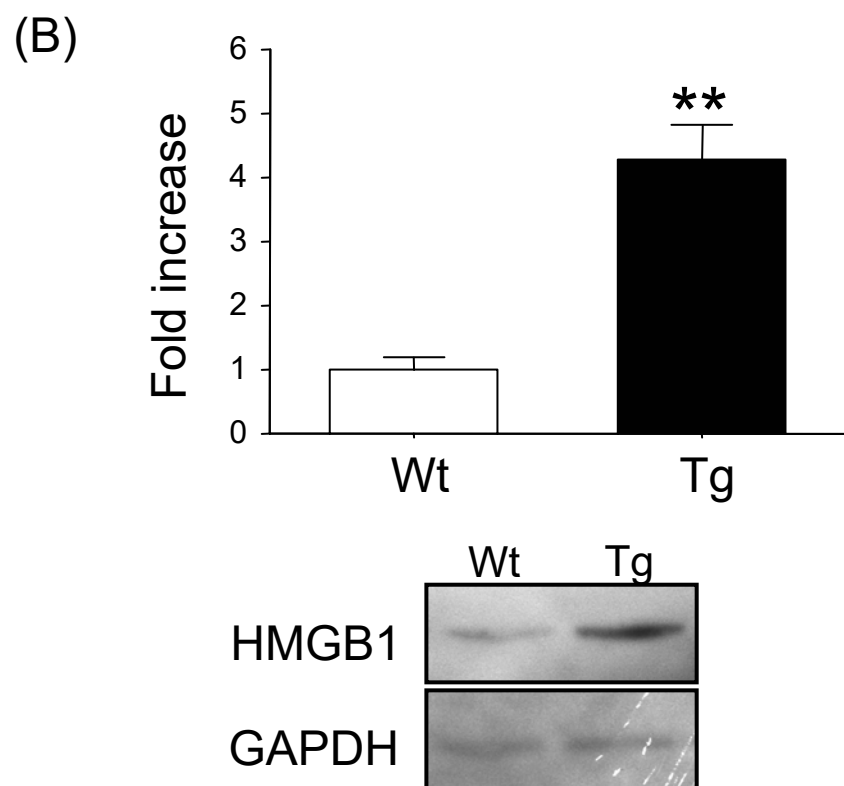


Figure 1

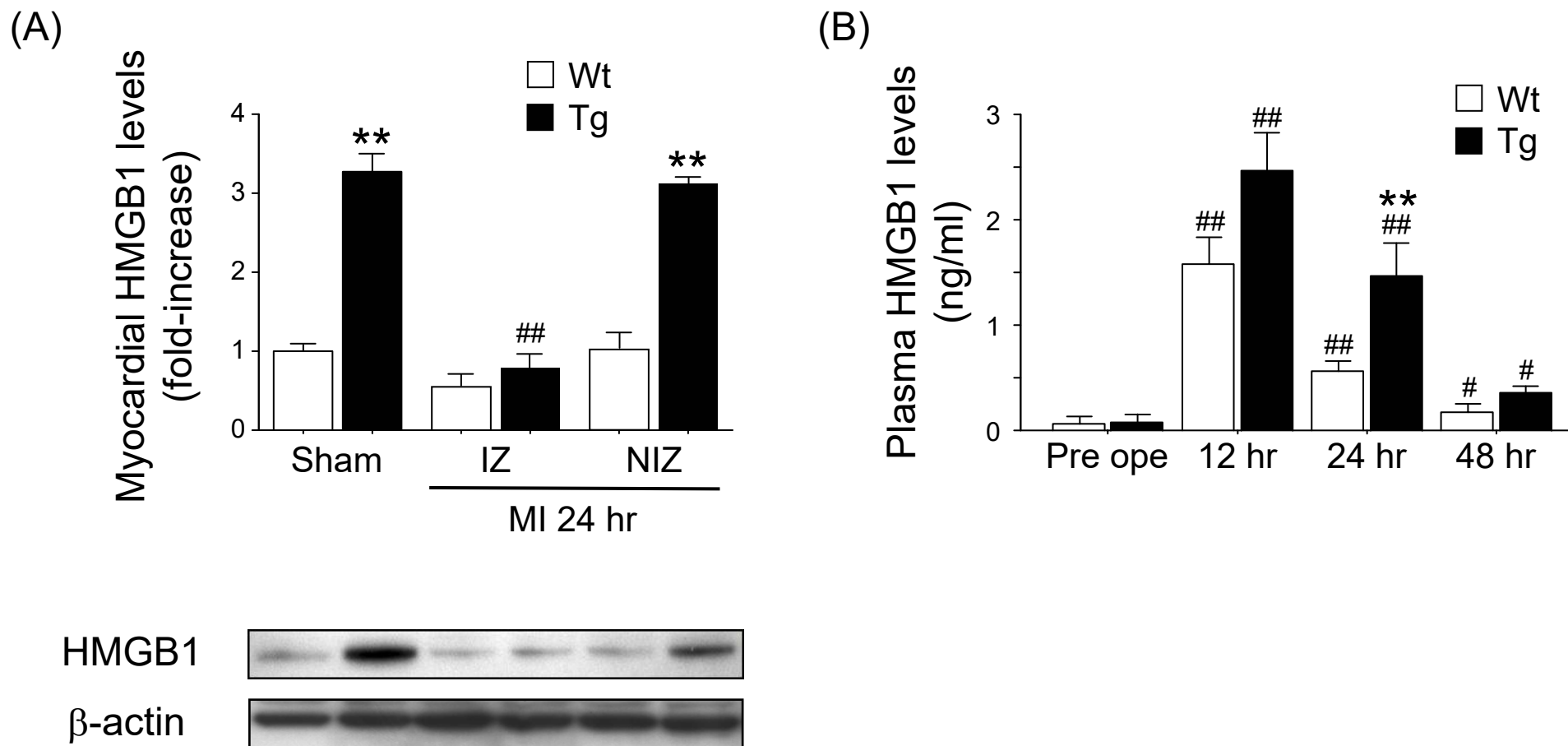


Figure 2

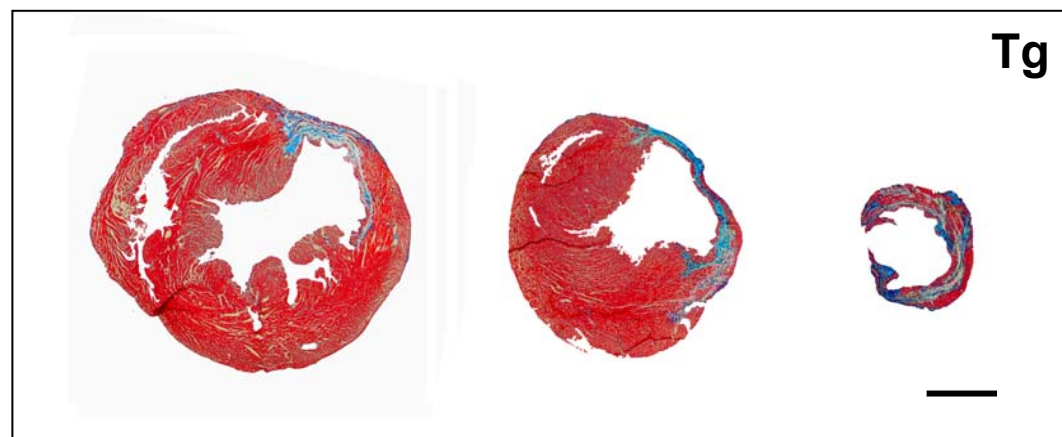
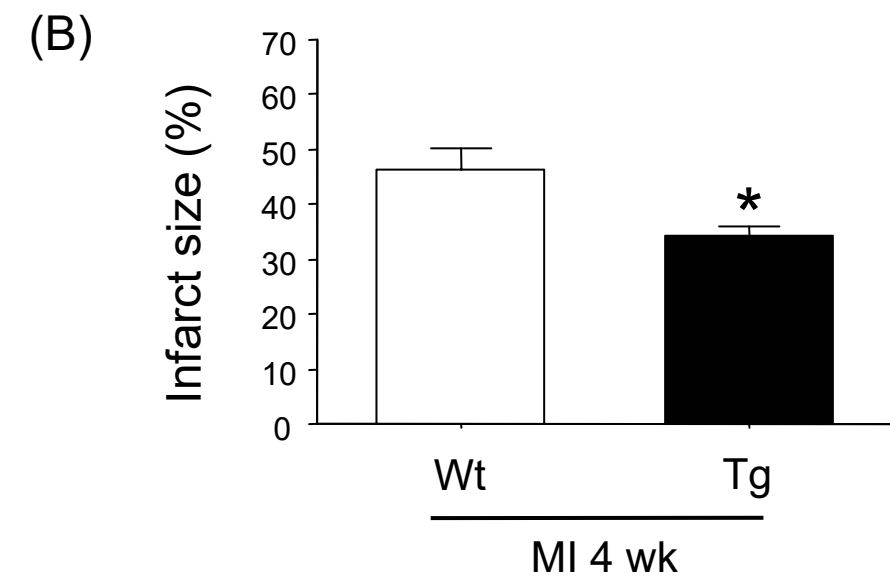
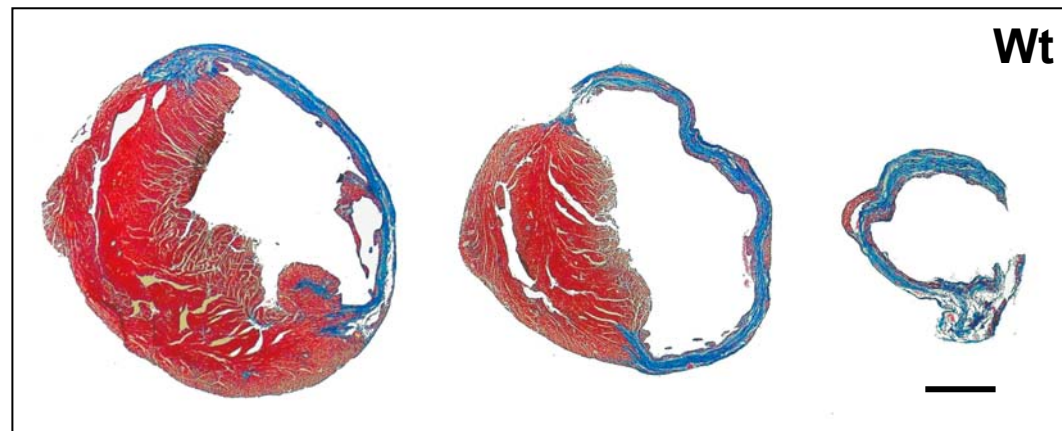
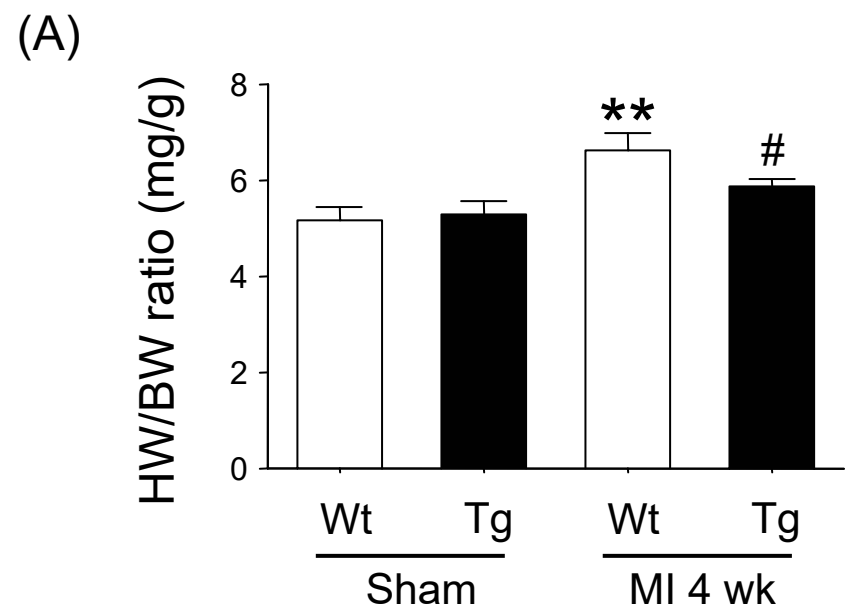


Figure 3

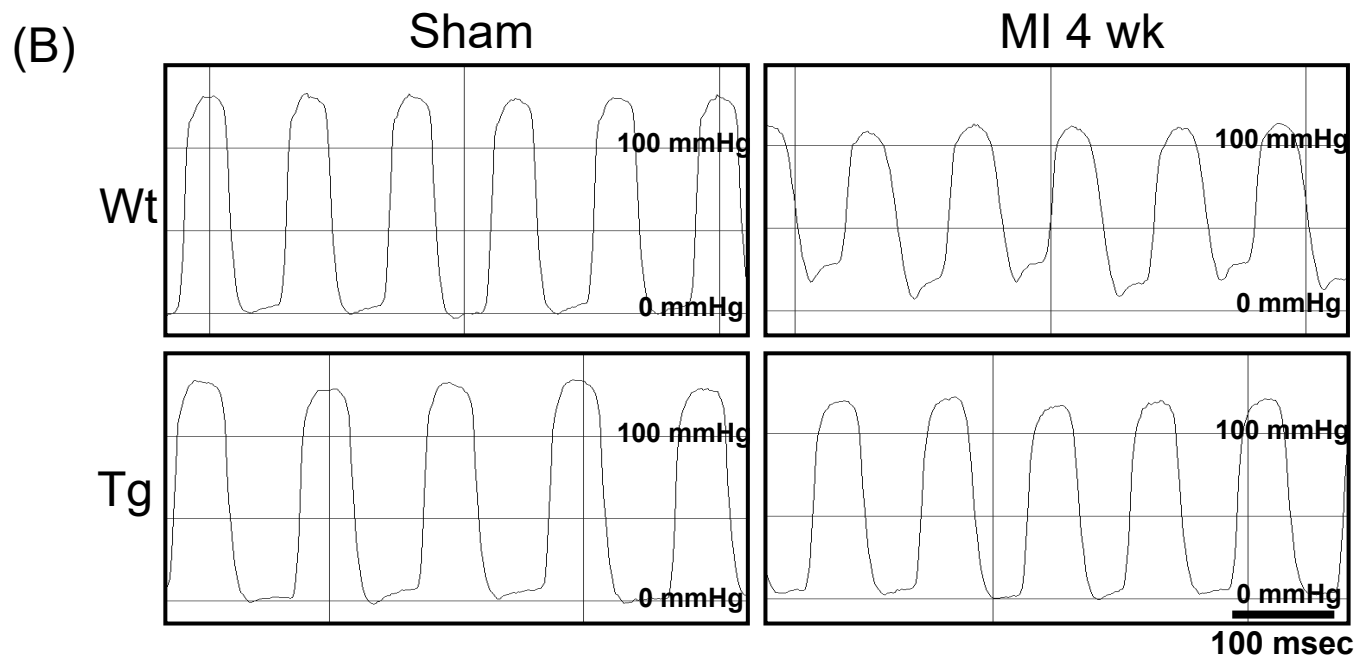
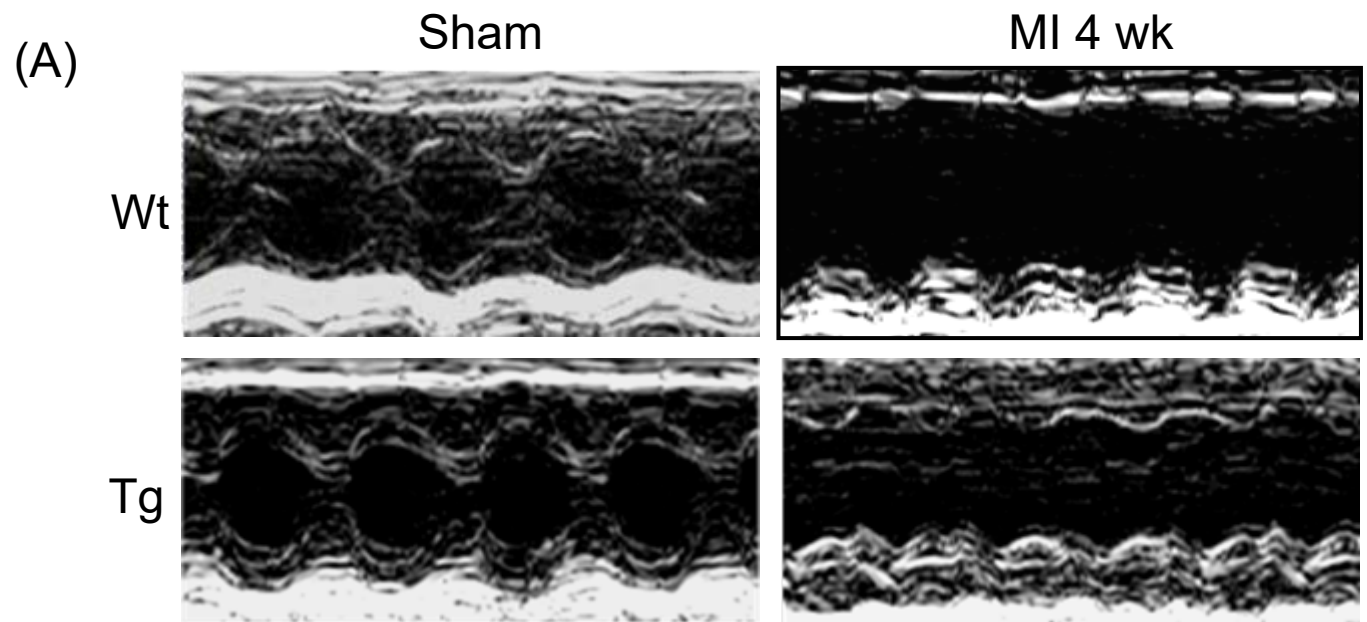


Figure 4

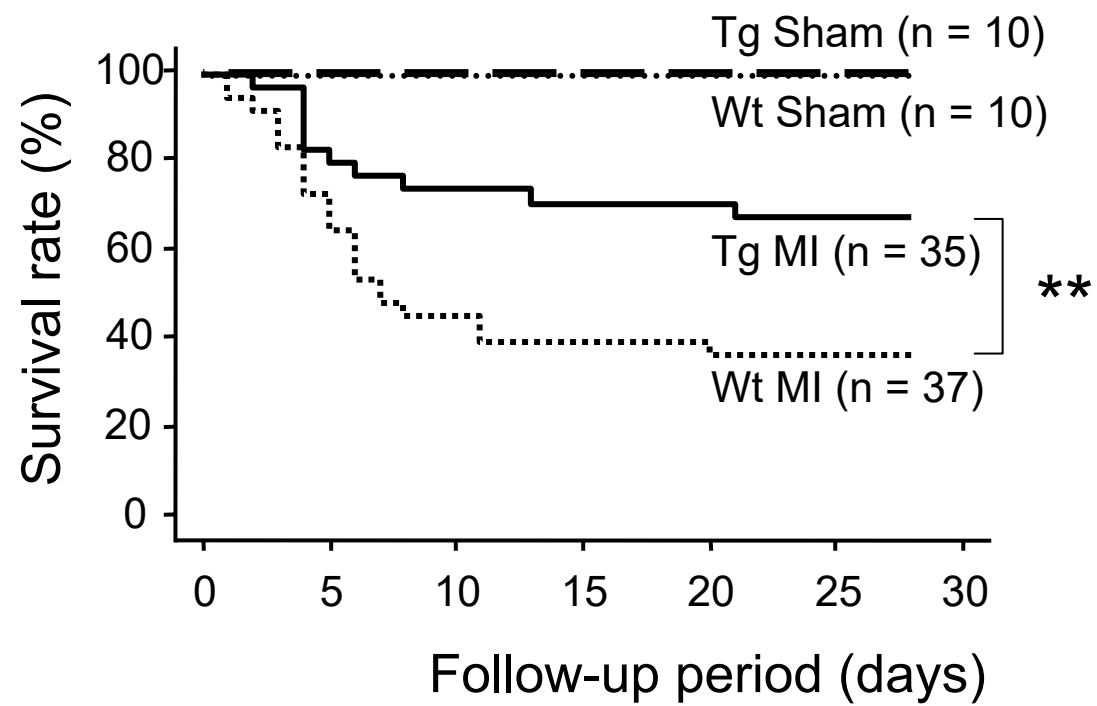


Figure 5

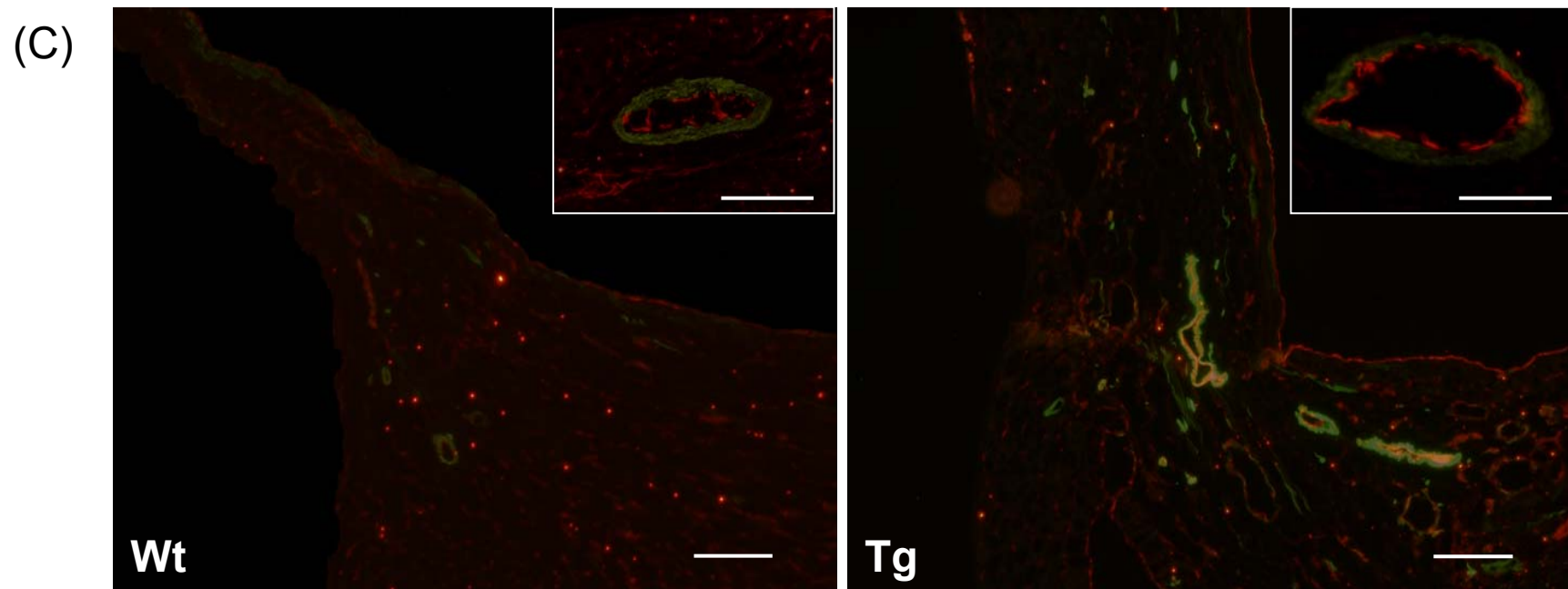
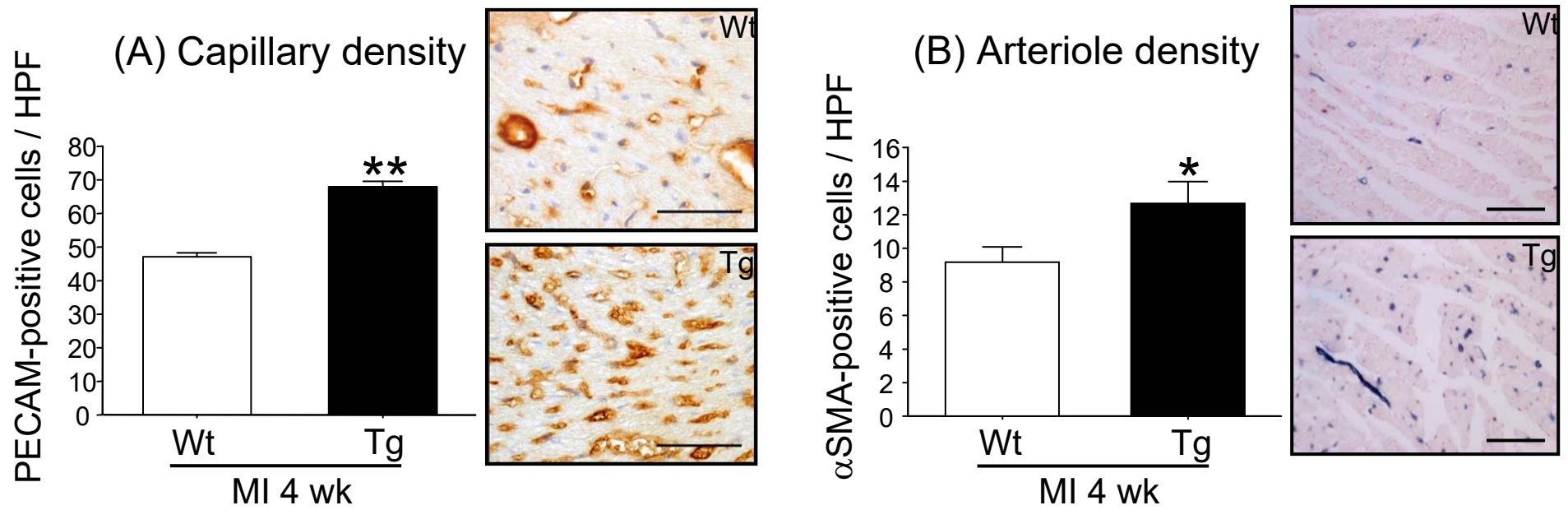


Figure 6